Journal of Organometallic Chemistry 902 (2019) 120968

Contents lists available at ScienceDirect

Journal of Organometallic Chemistry

journal homepage: www.elsevier.com/locate/jorganchem

# Synthesis, characterization and antitumor activity of novel ferrocene-coumarin conjugates

Jing-Na Wei, Zhao-Dong Jia, Yuan-Qing Zhou, Pei-Hua Chen, Biao Li, Ning Zhang, Xin-Qi Hao, Yan Xu*, Bin Zhang**

*The College of Chemistry, Zhengzhou University, Zhengzhou, 450001, Henan, PR China*

ARTICLE INFO

*Article history:*
Received 31 July 2019
Received in revised form
1 October 2019
Accepted 1 October 2019
Available online 2 October 2019

*Keywords:*
Ferrocene-coumarin conjugates
Crystal structure
Electrochemistry
Anticancer activity

ABSTRACT

Seven novel ferrocene-coumarin conjugates, namely **$FcL_1$~$FcL_7$**, were synthesized and confirmed by $^1H$ NMR, FT-IR, elemental analysis. The crystal structure of **$FcL_3$** was determined by X-ray diffraction, showing that the dihedral angle between the coumarin and the substituted cyclopentadienyl ring was 80.67°. The electrochemical behaviors of **$FcL_1$~$FcL_7$** exhibited similar quasireversible redox waves, while the formal potential $E^0$ values of **$FcL_1$~$FcL_5$** were distinctively lower than **$FcL_6$** and **$FcL_7$** due to electronic-effect of substituents. Notably, the title compounds, when screened on human tumor cell lines (MCF-7, BIU-87, SGC-7901, EC-9706, Eca-109 and Jurkat), exhibited potent and broad spectrum activities. Among them, **$FcL_1$~$FcL_5$** exhibited more toxicity to most cancer cell lines than **$FcL_6$** and **$FcL_7$** because of the lower $E^0$. Remarkably, **$FcL_4$** showed significant in vitro cytostatic effect on BIU-87 cell line giving respective $IC_{50}$ values of 1.09 μmol/L, which was much better than that of Adriamycin ($IC_{50} = 6.09$ μmol/L). The cytotoxicity assay against SGC-7901 cells also revealed that the complex **$FcL_5$** ($IC_{50} = 3.56$ μmol/L) was superior to the reference drug Adriamycin ($IC_{50} = 5.44$ μmol/L). Consequently, ferrocene-coumarin conjugates are potential candidates for developing metallodrugs with impressive anticancer activity.



## 1. Introduction

Coumarins (2H-1-benzopyran-2-one) can be found throughout the plant kingdom as well as bacteria, fungi, and marine sources [1–4], which have been demonstrated to possess diverse biological activities including antioxidant [5,6], antiinflammatory [7,8], antibacterial [9,10], anticancer activity [11–13], anti-HIV [14,15], ect.

However, natural coumarin has shortcomings such as low activity, poor fat solubility or low bioavailability, which limit its application [16,17]. Fortunately, coumarin has a large conjugated system and strong electron transfer ability, which make it easier to modify the structure and introduce various functional groups [18,19]. In past few years, a significant amount of effort has been invested to develop coumarin derivatives, which showed excellent therapeutic potency. For example, Hany A El-Sherief et al. have synthesized 4-methylcoumarin-chalcone hybrids and proved some of them with better anti-proliferative activity on MCF-7 [20]. Alessandra Bisi et al. have synthesized 7-hydroxycoumarin derivatives, some of them were confirmed with significant cytotoxicity on colon cancer cells [21]. Despite numerous effects of coumarins in the search for bioactive compounds, they still remain as one of the most versatile class of compounds for developing more effective and less toxic agents.

Ferrocene (Fc), a sandwich-like complex, possess exceptional redox properties [22,23], where oxidation to generate ferrocenium ($Fc^+$) species can facilitate the production of reactive oxygen species (ROS) [24,25]. It is well known that ROS in cancer cells induces oxidative damage to DNA and thus disturbs the cell cycle [26]. In addition to this, the remarkable biocompatibility (lipophilicity) property of ferrocene can alter the permeability of the compound [27]. As a result, ferrocene and its derivatives have been serving as cytotoxic agents against cancer cells, especially for hormone-dependent and hormone-independent breast cancer cells [24,28,29]. Meanwhile, the stability and aromaticity of Fc make it easily incorporate into the structure of other anticancer drugs to increase the activity. For instance, Xiomara Narváez-Pita et al. synthesized ferrocene-steroid conjugates and found that these conjugates displayed moderate to high anti-proliferative activity on colon cancer HT-29 and breast cancer MCF-7 cell lines [30]. José A.

* Corresponding author.
** Corresponding author.
*E-mail addresses:* xuyan@zzu.edu.cn (Y. Xu), bz@zzu.edu.cn (B. Zhang).

https://doi.org/10.1016/j.jorganchem.2019.120968
0022-328X/

Carmona-Negrón et al. have synthesized ferrocene-hormone conjugates and observed these compounds showed cytotoxic activity comparable to tamoxifen and cisplatin [24]. More recently, the combination of a ferrocenyl moiety and coumarin structures was found to significantly increase the biological activity [31].

Inspired by the recent upsurge in the use of ferrocene as an excellent additional to coumarin derivatives to enhance their antitumor activity, in this context, we designed and synthesized a series of new ferrocene-coumarin conjugates. These ferrocene-coumarin conjugates were evaluated for antitumor activity against the six human tumor cell lines, using Adriamycin as standard drug.

## 2. Experimental

### 2.1. Instruments and reagents

Melting points were measured using Beijing XT4B precision microscopic melting point apparatus. IR spectra were recorded on Bruker vector 22 infrared spectrometer with KBr pellets. $^1$H NMR and $^{13}$C NMR spectra were obtained on Bruker-Avance III-600 nuclear magnetic resonance instrument with tetramethylsilane (TMS) as the internal standard. C, N, and H analyses were performed on Flash EA 1112 elemental analyzer. All solvents were dried before use. Reagents and materials were purchased from commercial suppliers.

### 2.2. Synthesis of coumarin intermediates

The starting materials **$L_1$**, **$L_2$** were purchased from Aldric Co., and were used as recived. **$L_3$**, **$L_4$ and $L_5$** were synthesized according to the literature procedures [32–34].

### 2.3. Synthesis of ferrocene-coumarin conjugates

Ferrocene derivatives (3 mmol) and coumarin intermediate (3 mmol) were added into a 150 mL 3-necked flask, then 60 mL of methylene chloride (anhydrous treatment with calcium hydride) was introduced into the flask, stirred at room temperature until the solid dissolved, then a mixture of DAMP (0.15 mmol, 0.018 g) and DCC (3 mmol, 0.618 g) in $CH_2Cl_2$ (10 mL) was added dropwise. The reaction mixture was stirred at room temperature for 16 h and the progress of the reaction was monitored by TLC. After the reaction was completed, the reaction mixture was filtered and the filtrate was concentrated to get the crude products, which was purified by a silicagel column chromatography to give the pure products.

#### 2.3.1. 7-Hydroxycoumarin-ferrocene butyrate conjugate (***FcL$_1$***)

**$FcL_1$** jacinth solid was obtained by using column chromatography (ethyl acetate - petroleum ether, 1:2). Yield 68%; m.p. 99–100 °C. Anal. Calcd for $C_{23}H_{20}O_4Fe$ (%): C, 66.42; N, 0; H, 4.78. Found (%): C, 66.37; N, 0; H, 4.84. IR (KBr, cm$^{-1}$): 3097(w), 2936(w), 2852(w), 1767(s), 1723(s), 1694(m), 1615(s), 1561(m), 1500(w), 1424(w), 1100(s), 1056(m), 815(s). $^1$H NMR (DMSO, $\delta$, ppm): 8.08 (d, $J$ = 9.6 Hz, 1H, H–Ar), 7.78 (d, $J$ = 8.4 Hz, 1H, H–Ar), 7.28 (d, $J$ = 1.5 Hz, 1H, H–Ar), 7.17 (dd, $J$ = 8.4, 1.8 Hz, 1H, H–Ar), 6.48 (d, $J$ = 9.6 Hz, 1H, H–Ar), 4.13 (s, 7H, H-Fc), 4.07 (s, 2H, H-Fc), 2.65 (t, $J$ = 7.3 Hz, 2H, H–$CH_2$), 2.41 (t, $J$ = 7.1 Hz, 2H, H–$CH_2$), 1.88–1.83 (m, 2H, H–$CH_2$). $^{13}$C NMR (DMSO, $\delta$, ppm): 171.77, 160.18, 154.58, 153.36, 144.30, 129.82, 119.15, 117.13, 116.00, 110.59, 68.83, 68.30, 67.49, 33.62, 28.61, 25.83. MS (ESI) calculated for $C_{23}H_{20}O_4Fe$ [M+Na]$^+$ $m/z$: 439.00 found: 439.07.

#### 2.3.2. 4-Methyl-7-hydroxycoumarin-ferrocene butyrate conjugate (***FcL$_2$***)

**$FcL_2$** earthy yellow solid was obtained by using column chromatography (ethyl acetate - petroleum ether, 1:2). Yield 70%; m.p. 111–113 °C. Anal. Calcd for $C_{24}H_{22}O_4Fe$ (%): C, 67.00; N, 0; H, 5.13. Found (%): C, 66.99; N, 0; H, 5.15. IR (KBr, cm$^{-1}$): 3088(m), 2918(m), 2851(m), 1731(s), 1717(s), 1624(s), 1611(s), 1568(m), 1501(m), 1440(m), 1103(vs), 1067(s), 818(s). $^1$H NMR (DMSO, $\delta$, ppm): 7.82 (d, $J$ = 8.6 Hz, 1H, H–Ar), 7.27 (d, $J$ = 2.0 Hz, 1H, H–Ar), 7.19 (dd, $J$ = 8.6, 2.0 Hz, 1H, H–Ar), 6.39 (s, 1H, H–Ar), 4.13 (s, 7H, H-Fc), 4.07 (s, 2H, H-Fc), 2.66 (t, $J$ = 7.3 Hz, 2H, H–$CH_2$), 2.43 (s, 3H, H–$CH_3$), 2.41 (t, $J$ = 7.0 Hz, 2H, H–$CH_2$), 1.88–1.83 (m, 2H, H–$CH_2$). $^{13}$C NMR (DMSO, $\delta$, ppm): 171.77, 160.08, 154.01, 153.41, 153.36, 126.88, 118.90, 117.97, 114.20, 110.58, 68.83, 68.30, 67.49, 33.62, 28.62, 25.82, 18.64. MS (ESI) calculated for $C_{24}H_{22}O_4Fe$ [M+Na]$^+$ $m/z$: 453.00 found: 453.09.

#### 2.3.3. 7-Hydroxy-8-nitrocoumarin-ferrocene butyrate conjugate (***FcL$_3$***)

**$FcL_3$** earthy yellow solid was obtained by using column chromatography (ethyl acetate - petroleum ether, 1:1). Yield 50%; m.p. 126–127 °C. Anal. Calcd for $C_{23}H_{19}O_6NFe$ (%): C, 59.97; N, 3.10; H, 4.11. Found (%): C, 59.89; N, 3.04; H, 4.15. IR (KBr, cm$^{-1}$): 3084(w), 2925(w), 2850(w), 1786(s), 1741(m), 1622(m), 1540(m), 1434(w), 1110(w), 1066(m), 814(s). $^1$H NMR (DMSO, $\delta$, ppm): 8.17 (d, $J$ = 9.7 Hz, 1H, H–Ar), 8.05 (d, $J$ = 8.7 Hz, 1H, H–Ar), 7.50 (d, $J$ = 8.6 Hz, 1H, H–Ar), 6.65 (d, $J$ = 9.7 Hz, 1H, H–Ar), 4.13 (s, 7H, H-Fc), 4.07 (s, 2H, H-Fc), 2.68 (t, $J$ = 7.2 Hz, 2H, H–$CH_2$), 2.39 (t, $J$ = 7.0 Hz, 2H, H–$CH_2$), 1.85–1.80 (m, 2H, H–$CH_2$). $^{13}$C NMR (DMSO, $\delta$, ppm): 170.80, 157.98, 146.01, 144.19, 143.76, 132.02, 120.36, 118.55, 117.43, 68.84, 68.30, 67.53, 33.33, 28.43, 25.87. MS (ESI) calculated for $C_{23}H_{19}O_6NFe$ [M+Na]$^+$ $m/z$: 484.50 found: 484.06.

#### 2.3.4. 4-Methyl-7-hydroxy-8-nitrocoumarin-ferrocene butyrate conjugate (***FcL$_4$***)

**$FcL_4$** jacinth solid was obtained by using column chromatography (ethyl acetate - petroleum ether, 2:1). Yield 55%; m.p. 134–136 °C. Anal. Calcd for $C_{24}H_{21}O_6NFe$ (%): C, 60.70; N, 2.93; H, 4.42. Found (%): C, 60.65; N, 2.95; H, 4.45. IR (KBr, cm$^{-1}$): 3084(w), 2927(w), 2851(w), 1781(s), 1745(s), 1621(m), 1569(w), 1537(m), 1433(w), 1117(m), 1071(m), 820(m). $^1$H NMR (DMSO, $\delta$, ppm): 8.10 (d, $J$ = 8.8 Hz, 1H, H–Ar), 7.53 (d, $J$ = 8.8 Hz, 1H, H–Ar), 6.57 (s, 1H, H–Ar), 4.14 (s, 7H, H-Fc), 4.08 (s, 2H, H-Fc), 2.68 (t, $J$ = 7.0 Hz, 2H, H–$CH_2$), 2.48 (s, 3H, H–$CH_3$), 2.38 (t, $J$ = 7.1 Hz, 2H, H–$CH_2$), 1.84–1.81 (m, 2H, H–$CH_2$). $^{13}$C NMR (DMSO, $\delta$, ppm): 170.78, 157.83, 153.17, 145.44, 144.12, 132.23, 129.14, 120.04, 119.40, 115.28, 68.87, 68.32, 67.57, 33.35, 28.44, 25.86, 18.79. MS (ESI) calculated for $C_{24}H_{21}O_6NFe$ [M+Na]$^+$ $m/z$: 498.00 found: 498.07.

#### 2.3.5. 7-Aminocoumarin-ferrocene butyrate conjugate (***FcL$_5$***)

**$FcL_5$** jacinth solid was obtained by using column chromatography (ethyl acetate - petroleum ether, 1:1). Yield 51%; m.p. 136–138 °C. Anal. Calcd for $C_{23}H_{21}O_3NFe$ (%): C, 66.56; N, 3.35; H, 5.13. Found (%): C, 66.52; N, 3.37; H, 5.10. IR (KBr, cm$^{-1}$): 3315(m), 3087(w), 2932(m), 2851(w), 1717(s), 1662(s), 1619(m), 1574(s), 1551(s), 1487(m), 1439(s), 1100(s), 1040(s), 818(s). $^1$H NMR (DMSO, $\delta$, ppm): 8.05 (s, 1H, H–NH), 7.68 (d, $J$ = 9.2 Hz, 2H, H–Ar), 7.41 (d, $J$ = 8.7 Hz, 1H, H–Ar), 7.25 (d, $J$ = 8.8 Hz, 1H, H–Ar), 6.43 (d, $J$ = 9.5 Hz, 1H, H–Ar), 4.13 (s, 5H, H-Fc), 4.10 (s, 2H, H-Fc), 4.08 (s, 2H, H-Fc), 2.43 (t, $J$ = 7.4 Hz, 2H, H–$CH_2$), 2.39 (t, $J$ = 7.3 Hz, 2H, H–$CH_2$), 1.94–1.89 (m, 2H, H–$CH_2$). $^{13}$C NMR (DMSO, $\delta$, ppm): 171.51, 160.91, 150.29, 143.63, 134.68, 123.50, 119.00, 118.40, 117.15, 117.10, 69.27, 68.71, 67.89, 36.88, 29.02, 26.65. MS (ESI) calculated for $C_{23}H_{21}O_3NFe$ [M+Na]$^+$ $m/z$: 438.00 found: 438.09.

#### 2.3.6. 7-Hydroxycoumarin-Ferrocene formyl propionic acid conjugate (**FcL$_6$**)

**FcL$_6$** brown solid was obtained by using column chromatography (dichloromethane - ethyl acetate, 16:1). Yield 70%; m.p. 151–152 °C. Anal. Calcd for $C_{23}H_{18}O_5Fe$ (%): C, 64.42; N, 0; H, 4.23. Found (%): C, 64.21; N, 0; H, 4.22. IR (KBr, $cm^{-1}$): 3085(w), 2913(w), 1723(s), 1668(s), 1615(s), 1564(m), 1499(w), 1451(m), 1119(s), 1086(s), 824(s). $^1$H NMR (DMSO, $\delta$, ppm): 8.07 (d, $J$ = 9.5 Hz, 1H, H–Ar), 7.79 (d, $J$ = 8.4 Hz, 1H, H–Ar), 7.16–7.24 (m, 2H, H–Ar), 6.47 (d, $J$ = 9.5 Hz, 1H, H–Ar), 4.86 (s, 2H, H-Fc), 4.58 (s, 2H, H-Fc), 4.26 (s, 5H, H-Fc), 3.20 (t, $J$ = 6.0 Hz, 2H, H–$CH_2$), 2.90 (t, $J$ = 6.0 Hz, 2H, H–$CH_2$). $^{13}$C NMR (DMSO, $\delta$, ppm): 202.03, 171.79, 160.16, 154.59, 153.47, 144.30, 129.92, 119.03, 117.13, 116.02, 110.38, 78.65, 72.62, 70.15, 69.51, 34.37, 28.27. MS (ESI) calculated for $C_{23}H_{18}O_5Fe$ $[M+H]^+$ $m/z$: 431.00 found: 431.05.

#### 2.3.7. 4-Methyl-7-hydroxycoumarin-Ferrocene formyl propionic acid conjugate (**FcL$_7$**)

**FcL$_7$** brown solid was obtained by using column chromatography (dichloromethane - ethyl acetate, 16:1). Yield 75%; m.p. 164–167 °C. Anal. Calcd for $C_{24}H_{20}O_5Fe$ (%): C, 64.90; N, 0; H, 4.57. Found (%): C, 64.89; N, 0; H, 4.54. IR (KBr, $cm^{-1}$): 3090(m), 2927(w), 1722(s), 1664(s), 1611(s), 1573(m), 1501(m), 1457(m), 1105(vs), 1092(s), 827(s). $^1$H NMR (DMSO, $\delta$, ppm): 7.83–7.85 (m, 1H, H–Ar), 7.24 (s, 1H, H–Ar), 7.18 (d, $J$ = 8.4 Hz, 1H, H–Ar), 6.39 (s, 1H, H–Ar), 4.86 (s, 2H, H-Fc), 4.59 (s, 2H, H-Fc), 4.26 (m, 5H, H-Fc), 3.21 (t, $J$ = 6.2 Hz, 2H, H–$CH_2$), 2.91 (t, $J$ = 6.0 Hz, 2H, H–$CH_2$), 2.43 (s, 3H, H–$CH_3$). $^{13}$C NMR (DMSO, $\delta$, ppm): 202.03, 171.78, 160.07, 154.03, 153.48, 153.42, 127.00, 118.79, 117.97, 114.20, 110.36, 78.66, 72.62, 70.15, 69.51, 34.38, 28.27, 18.64. MS (ESI) calculated for $C_{24}H_{20}O_5Fe$ $[M+Na]^+$ $m/z$: 467.00 found: 467.07.

### 2.4. Crystal structure determination

The crystal of **FcL$_3$** suitable for X-ray analysis was obtained by slow evaporation from the mixed solvent ($V$**CHCl$_3$**:$V$**C$_2$H$_5$OH** = 1:3) at room temperature. Single crystal X-ray distraction data of **FcL$_3$** were collected at 293(2) K on a Bruker SMART APEX IICCD with graphite monochromated MoK radiation ($\lambda$ = 0.71073 Å) in $\omega$ scan mode. The structure was solved by the direct method using *SHELXT-2014* and expanded using Fourier techniques. Non-H atoms were refined using the riding model by the full-matrix least-squares procedure based on $F^2$ values.

### 2.5. Electrochemical measurements

Electrochemistry experiments were measured via an RST5000 electrochemical workstation, equipped with three-electrode system, taking glassy carbon electrode as working electrode, platinum wire electrode as counter electrode, saturated $Hg/Hg_2Cl_2$ electrode as reference electrode. The electrochemical properties of the target compounds **FcL$_1$~FcL$_7$** were investigated by cyclic voltammetry in acetonitrile ($CH_3CN$) with tetrabutylammonium perchlorate (0.1 mol/L) as the supporting electrolyte. Cyclic voltammetry (CV) of the **FcL$_1$~FcL$_7$** was performed over a potential from −0.2 to 0.8 V at different scanning rates (100 mV/s, 200 mV/s, 300 mV/s, 400 mV/s, 500 mV/s). The potentials were reported in volts using the $Fc/Fc^+$ couple as reference.

### 2.6. Anticancer activity measurements

Human bladder cancer cell line (BIU-87),human gastric cancer cell line (SGC-7901),human esophageal cancer cell line (EC-9706 and Eca-109), human breast cancer cell line (MCF-7),human leukemia cell line (Jurkat) were cultured as test cancer cells for anticancer activity experiment.

The compounds **FcL$_1$~FcL$_7$** were solubilized in DMSO at a concentration of 4 mg/mL and then were diluted to 40,20,10,5,2.5 μg/mL with ROMI-1640. 100 μL human cell lines ($7.5 \times 10^3$–$8.0 \times 10^3$ cells per well) were added into 96-well plates for 24 h under a suitable atmosphere containing 5% $CO_2$ at 37 °C. Equivalent volumes of **FcL$_1$~FcL$_7$** with different concentrations were poured into the culture, then, the cells were incubated for 24 h under the same condition. After 24 h, 5 μL CCK8 reagent was added and cells were incubated for another 4 h at 37 °C. The absorbance of each well was read at 450 nm (OD450) with a microplate reader. $IC_{50}$ values were determined using SPSS software.

## 3. Results and discussion

### 3.1. Synthesis and structural characterization

The Fc-functionalized coumarin conjugates were synthesized via reaction between ferrocene derivatives and coumarin intermediates in the presence of DCC/DMAP under an inert (Ar) atmosphere (Schemes 1–3). The chemical structures of the newly synthesized compounds were fully characterized by FT-IR, $^1$H NMR, $^{13}$C NMR and elemental analysis, which were in good accordance with the proposed structures.

The FT-IR spectra of the complexes **FcL$_1$~FcL$_4$**, **FcL$_6$** and **FcL$_7$** showed characteristic –C=O- and -C-O- stretching vibrations in the ranges 1717–1745 and 1100-1119 $cm^{-1}$, respectively. Meanwhile, the absorptions arising for the amide group at 1551 (-N-C = , s), 1662 (-C=O, s) and 3315 (-N-H, m) $cm^{-1}$. These spectroscopic data clearly confirmed that the ferrocene group was successfully incorporated to the coumarin backbone via ester/amide linkage. Additionally, the characteristic absorptions of Fc were appeared at 1424–1457,1040–1092, 814–827 $cm^{-1}$, which are similar to previous reports [35]. Coumarin displayed characteristic absorptions at 3084–3097,1717–1786, 1615–1624 $cm^{-1}$, which agree with previous reports very well [11,36].

Several $^1$H NMR and $^{13}$C NMR features evinced the **FcL$_1$~FcL$_7$** structure that were presented in Figs. S1–S14 in the Supporting Information. The $^1$H NMR spectra exhibited similar resonances for the protons of coumarin skeleton, falling in the range $\delta$ 6.39–8.17 [37,38]. The $^1$H NMR signals of **FcL$_1$~FcL$_4$** showed two signal sets at $\delta$ 4.13–4.14 (7H) and $\delta$ 4.07–4.08 (2H) for the ferrocene fragments [39]. Resonances for the protons of Fc fragment in **FcL$_5$** were located at $\delta$ 4.13 (s, 5H), $\delta$ 4.10 (s, 2H) and $\delta$ 4.08 (s, 2H). The chemical shift of the ferrocene in **FcL$_6$** and **FcL$_7$** were positively shifted at $\delta$ 4.86 (2H), $\delta$ 4.58–4.59 (2H) and $\delta$ 4.26 (5H) due to the electron-withdrawing effect of the carbonyl group. Additionally, all these **FcL$_X$** (x = 1–7) exhibited signals in the regime $\delta$ 1.80–3.21 assigned to the methylene and methyl protons. The resonance peaks with the chemical shift at $\delta$ 8.05 could be ascribed to protons near the N atom on the amide of **FcL$_5$**.

### 3.2. Crystal structures analysis

The solid structure of complex **FcL$_3$** was characterized by single-crystal X-ray diffraction (Fig. 1). The crystallographic details are presented in Table 1. Selected bond lengths and dihedral angles are summarized in Table 2. The bond lengths of ferrous ions and each carbon atom of the cyclopentadienyl ring (Cp) were ranged from 2.025(2) to 2.047(2) Å, which are similar to the analogous ferrocene derivatives [40]. Meanwhile, the dihedral angle between the substituted and unsubstituted Cp rings was only 1.31°, suggesting that the two Cp rings were almost parallel to each other. Compared with other similar compounds [41], the bond lengths of the

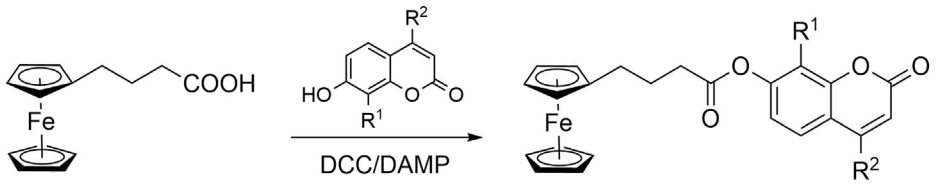


**Scheme 1.** Synthesis of the ferrocene-coumarin conjugates **$FcL_1$~$FcL_4$**.

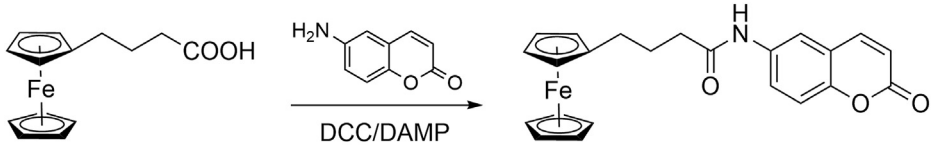


**Scheme 2.** Synthesis of the ferrocene-coumarin conjugate **$FcL_5$**.

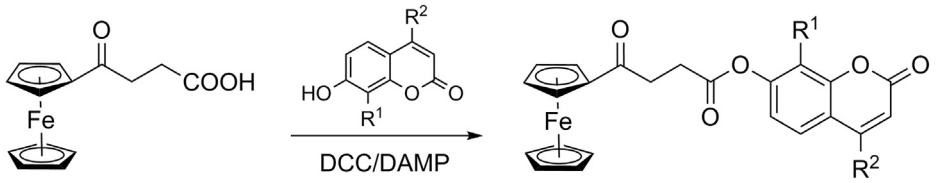


**Scheme 3.** Synthesis of the ferrocene-coumarin conjugates **$FcL_6$** and **$FcL_7$**.

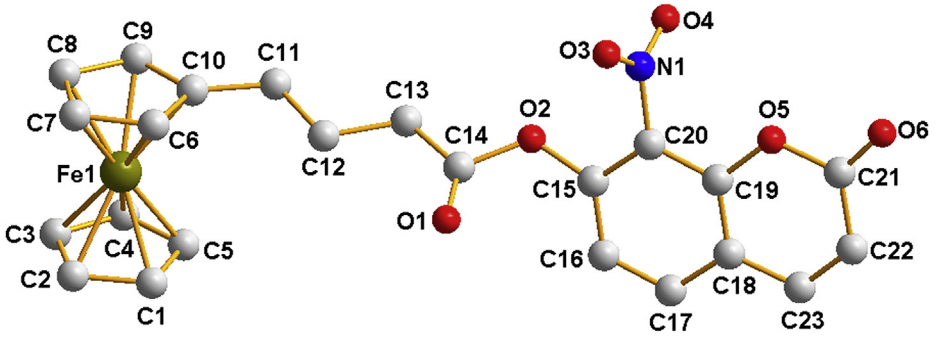


**Fig. 1.** X-ray crystal structure of compound **$FcL_3$** and all hydrogen atoms are omitted for clarity.

coumarin derivatives were within the normal range. Notably, the non-hydrogen atoms on the coumarin moiety were coplanar and the dihedral angle between the plane of coumarin and the substituted cyclopentadienyl ring was 80.67°.

### 3.3. Electrochemical behavior analysis

Previous mechanistic studies have established a relationship between the DNA damage capability and the $Fc^{+/0}$ reduction potential of the ferrocenyl moieties, with lower $E^0$ values resulting in higher cytotoxicity [24,25]. The electrochemical behaviors of the compounds **$FcL_1$~$FcL_7$** were measured by cyclic voltammetry experiments using a three-electrode cell and compared to the ferrocene/ferrocenium redox couple in $CH_3CN$. The cyclic voltammograms (CV) of the compounds exhibited similar one-electron quasireversible waves, which could be assigned to the $Fc/Fc^+$. As shown in Table 3, the formal potentials ($E^0$) of **$FcL_1$~$FcL_5$** were lower ($E^0 \leq 0.352$) than pure ferrocene ($E^0 = 0.437$ V) due to the inductive electron-donation capacity of the methylene group [42]. On the other hand, the introduction a carbonyl group into the Cp resulted in higher $E^0$ of 0.637 and 0.632 V for **$FcL_6$** and **$FcL_7$**, respectively.

Additionally, the CV behaviors of **$FcL_1$~$FcL_7$** at different sweep rates (100−500 mV/s) were shown in Figs. S15−S20 and Fig. 2. As all compounds had the similar properties, **$FcL_3$** was elected as a representative for discussion. It is observed that the changes of the cathodic and anodic peak potentials could be ignored with increasing of scan rate, resulting in nearly same ΔE, meanwhile, the $i_{pa}/i_{pc}$ values were closed to unity. These phenomena indicated that the electrode reaction was reversible and ferrocene subunits were in an equivalent environment [43]. Furthermore, the current peak ($i_p$) increased linearly with the square root of the scan rate ($\nu^{1/2}$) (Fig. 3), which confirmed that the charge transfer process was diffusion-controlled [44]. Other compounds also showed the similar linear relationship between $i_p$ and $\nu^{1/2}$ (Figs. S21−S26).

### 3.4. Anticancer activity analysis

The anticancer activities of **$FcL_1$~$FcL_7$** were evaluated by a Cell Counting Kit8 (CCK-8) assay using a panel of six human cancer cell

**Table 1**
Crystal data and structure refinement of **$FcL_3$**.

| Empirical Formula | $C_{23}H_{19}FeNO_6$ |
|---|---|
| Formula weight | 461.24 |
| T (K) | 273.15 |
| Crystal system | Triclinic |
| Space group | *P*−1 |
| *a*/Å | 8.2960(3) |
| *b*/Å | 11.2106(4) |
| *c*/Å | 11.7280(4) |
| *α*/° | 103.582(2) |
| *β*/° | 93.9930(10) |
| *γ*/° | 102.3120(10) |
| *V*/Å$^3$ | 1027.59(6) |
| Z | 2 |
| ρ calcg/cm$^3$ | 1.491 |
| *μ*/mm$^{-1}$ | 0.775 |
| *F*/000 | 476.0 |
| *θ* range/° | 4.546 to 52 |
| Index ranges | $-10 \le h \le 10$, $-13 \le k \le 13$, $-14 \le l \le 14$ |
| Independent reflections | 4018 [$R_{int} = 0.0268$, $R_{sigma} = 0.0232$] |
| Data/restraints/parameters | 4018/12/280 |
| Final R indexes [$I \ge 2\sigma$ (I)] | $R_1 = 0.0327$, $wR_2 = 0.0855$ |
| Final R indexes [all data] | $R_1 = 0.0379$, $wR_2 = 0.0888$ |
| CCDC | 1912608 |

**Table 2**
Selected bond lengths (Å) and angles (°) for **$FcL_3$**.

| | | | |
|---|---|---|---|
| Fe(1)−C(1) | 2.047(2) | Fe(1)−C(2) | 2.036(2) |
| Fe(1)−C(3) | 2.025(2) | Fe(1)−C(4) | 2.026(2) |
| Fe(1)−C(5) | 2.038(2) | Fe(1)−C(6) | 2.039(2) |
| Fe(1)−C(7) | 2.035(2) | Fe(1)−C(8) | 2.037(2) |
| Fe(1)−C(9) | 2.038(2) | Fe(1)−C(10) | 2.047(2) |
| O(1)−C(14) | 1.179(3) | O(2)−C(14) | 1.393(2) |
| O(2)−C(15) | 1.382(2) | O(3)−N(1) | 1.188(3) |
| O(4)−N(1) | 1.172(3) | O(5)−C(19) | 1.365(2) |
| O(5)−C(21) | 1.390(2) | O(6)−C(21) | 1.200(2) |
| C(19)−C(20) | 1.388(3) | C(20)−N(1) | 1.462(2) |
| C(1)-Fe(1)-C(2) | 40.50(10) | C(1)-Fe(1)-C(3) | 68.24(11) |
| C(1)-Fe(1)-C(6) | 108.58(10) | C(2)-Fe(1)-C(4) | 68.07(12) |
| C(2)-Fe(1)-C(6) | 122.09(11) | C(2)-Fe(1)-C(8) | 124.91(10) |
| C(3)-Fe(1)-C(8) | 107.14(10) | C(3)-Fe(1)-C(10) | 161.34(11) |
| C(4)-Fe(1)-C(9) | 106.99(10) | C(5)-Fe(1)-C(10) | 106.99(9) |
| C(13)-C(14)-O(1) | 129.2(2) | C(14)-O(2)-C(15) | 120.29(16) |
| C(19)-O(5)-C(21) | 120.95(14) | O(1)-C(14)-O(2) | 122.19(19) |
| O(3)-N(1)-O(4) | 123.3(2) | O(3)-N(1)-C(20) | 118.80(18) |
| O(4)-N(1)-C(20) | 117.9(2) | O(5)-C(21)-O(6) | 115.58(19) |

**Table 3**
Cyclic voltammetry data of **Fc** and **$FcL_1$~$FcL_7$**.

| Compound | $E_{pc}$/V | $E_{pa}$/V | $E^0$/V | $\Delta E$/V | $i_{pa}/i_{pc}$ |
|---|---|---|---|---|---|
| Fc | 0.473 | 0.400 | 0.437 | 0.073 | 1.000 |
| $FcL_1$ | 0.384 | 0.318 | 0.351 | 0.066 | 1.098 |
| $FcL_2$ | 0.381 | 0.319 | 0.350 | 0.062 | 1.146 |
| $FcL_3$ | 0.384 | 0.319 | 0.352 | 0.065 | 1.200 |
| $FcL_4$ | 0.383 | 0.317 | 0.350 | 0.066 | 1.110 |
| $FcL_5$ | 0.373 | 0.305 | 0.339 | 0.068 | 1.052 |
| $FcL_6$ | 0.669 | 0.604 | 0.637 | 0.065 | 1.254 |
| $FcL_7$ | 0.665 | 0.598 | 0.632 | 0.067 | 1.271 |

lines: BIU-87 (Human bladder cancer cell), SGC-7901 (human gastric cancer cell), EC-9706 and Eca-109 (human esophageal cancer cell), MCF-7 (human breast adenocarcinoma cell) and Jurkat (human leukemia cell). The concentration ($IC_{50}$) of the complexes at which 50% of tumor cells were inhibited from proliferation was calculated.

From the $IC_{50}$ values collected in Table 4, the anticancer activities of **$FcL_1$~$FcL_5$** against MCF-7 with $IC_{50}$ in the range of 12.10−28.10 μmol/L were substantially better than that of **$FcL_6$** and

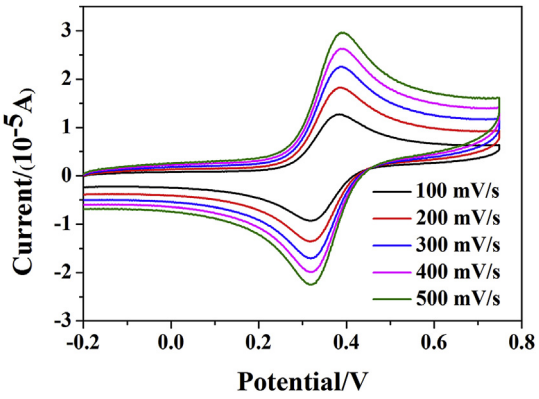


**Fig. 2.** The CV curves of **$FcL_3$** in $CNCH_3$

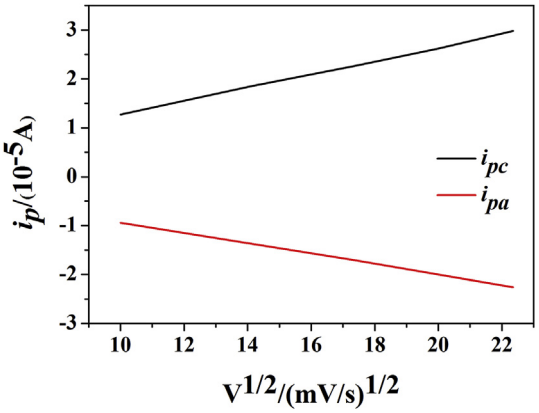


**Fig. 3.** The dependence $i_p$ vs. $V_{1/2}$ at different rates. (**$FcL_3$**).

**Table 4**
$IC_{50}$ values (μmol/L) of **$FcL_1$~$FcL_7$** and Adriamycin.

| Compound | BIU-87 | SGC-7901 | EC-9706 | Eca-109 | MCF-7 | Jurkat |
|---|---|---|---|---|---|---|
| $FcL_1$ | 5.24 | 7.46 | 82.83 | 42.47 | 28.10 | 55.77 |
| $FcL_2$ | 4.48 | 16.61 | 41.26 | 27.97 | 15.34 | 54.90 |
| $FcL_3$ | 15.27 | 19.78 | N | 40.00 | 23.91 | 38.38 |
| $FcL_4$ | 1.09 | 10.61 | 25.89 | 36.38 | 12.10 | 53.01 |
| $FcL_5$ | 18.45 | 3.56 | 45.58 | 18.64 | 20.88 | 35.66 |
| $FcL_6$ | 40.96 | N | N | 34.73 | 55.46 | 64.50 |
| $FcL_7$ | 37.10 | 62.57 | 40.35 | 16.64 | 50.27 | 63.96 |
| Adriamycin | 6.09 | 5.44 | 8.56 | 6.52 | 7.95 | 4.50 |

N represents $IC_{50}$ value greater than 100: no activity.

**$FcL_7$** ($IC_{50} > 50$ μmol/L). Similarly, for BIU-87, SGC-7901 and Jurkat, **$FcL_1$~$FcL_5$** also showed better anticancer activity than **$FcL_6$** and **$FcL_7$**. These phenomena indicated that the high anticancer activities of these complexes were related to their low $E^0$ values. Additionally, as a result of synergistic anticancer efficacies of coumarin moties together with a small difference of $E^0$, the $IC_{50}$ values were not correlate to the $E^0$ values of the **$FcL_1$~$FcL_5$** very well. For human esophageal cancer cell EC-9706 and Eca-109, the $IC_{50}$ values were not correlate to the $E^0$ values, which may be due to that the ferrocene moiety did not have the significant antiproliferative activity on these cancer cells.

Remarkably, the ferrocene-coumarin conjugates showed significant cytotoxicity toward the BIU-87 cell line, giving $IC_{50}$ of 1.09−40.96 μmol/L. Especially, the $IC_{50}$ values of compound **$FcL_1$**, **$FcL_2$** and **$FcL_4$** were 5.24, 4.48 and 1.09 μmol/L respectively, which were better than the standard Adriamycin ($IC_{50} = 6.09$ μmol/L).

These results demonstrated that the complexes were promising candidates for the development of cytotoxic drugs against bladder cancer cells. All the compounds also showed outstanding inhibitory activity against SGC-7901 with a lowest $IC_{50}$ value of 3.56 μmol/L (**$FcL_5$**). However, for EC-9706, Eca-109 and Jurkat cell lines, ferrocene-coumarin conjugates showed moderate to low cytotoxic activity on cancer cells.

The structure-activity relationship (SAR) analysis revealed that introduction of the methyl at C-4 position of coumarin had a beneficial influence on anticancer activity of the ferrocene-coumarin conjugatessite. For example, for BIU-87, EC-9706, Eca-109 and MCF-7, compounds **$FcL_2$**, **$FcL_4$** and **$FcL_7$** containing methyl group displayed a lower $IC_{50}$ than compounds **$FcL_1$**, **$FcL_3$** and **$FcL_6$**, respectively. For SGC-7901, compounds **$FcL_4$** and **$FcL_7$** also showed better antiproliferative activity in comparison to compounds **$FcL_3$** and **$FcL_6$**, respectively. Since compounds **$FcL_5$** showed better anticancer activity in comparison to compounds **$FcL_1$** for the cancer cell lines (except for BIU-87), the amide linkage is more effective to enhance anticancer activity than the ester linkage.

## 4. Conclusions

A series of ferrocene-coumarin conjugates (**$FcL_1$~$FcL_7$**) were synthesized. Cyclic voltammetry analyses revealed that the $E^0$ values of **$FcL_1$~$FcL_5$** were lower than that of **$FcL_6$** and **$FcL_7$**, which made **$FcL_1$~$FcL_5$** exhibited higher cytotoxicity toward most cancer cells. Importantly, the complexes **$FcL_1$**, **$FcL_2$** and **$FcL_4$** displayed more promising cytotoxic activity against BIU-87 cell line ($IC_{50} \leq 5.24$ μmol/L) than that of the standard Adriamycin ($IC_{50} = 6.09$ μmol/L). Specially, **$FcL_4$** with $IC_{50}$ value of 1.09 μmol/L was the most potent compound against BIU-87. The cytotoxicity assay against SGC-7901 cells revealed that the complex **$FcL_5$** ($IC_{50} = 3.56$ μmol/L) was more potent than the reference drug Adriamycin ($IC_{50} = 5.44$ μmol/L). In addition to this, the differences in the cytotoxic activities of these complexes suggested that the different substituents could be a viable approach for the development of new and more effective therapeutic agents. Consequently, these metal complexes can be lead in the development of potential specific-target inhibitors in cancer therapy.

## Declaration of competing interest

The authors declare no conflict of interest.

## Acknowledgements

We gratefully acknowledge the financial support of the National Natural Science Foundation of China (No. 21601156, 21171149).

## Appendix A. Supplementary data

Crystallographic data have been deposited with the Cambridge Crystallographic Data Centre as supplementary publication no. CCDC 1912608. Crystallographic data is available.

Supplementary data to this article can be found online at https://doi.org/10.1016/j.jorganchem.2019.120968.

## References

[1] S.G. Narellaa, M.G. Shaika, A. Mohammeda, M. Alvalaa, A. Angelib, C.T. Supuran, Bioorg. Chem. 87 (2019) 765–772.
[2] P. Bhavya, R. Melavanki, R. Kusanur, K. Sharma, V.T. Muttannavar, L.R. Naik, Luminescence 33 (2018) 933–940.
[3] H.M. Revankar, S.N.A. Bukhari, G.B. Kumar, H.L. Qin, Bioorg. Chem. 71 (2017) 146–159.
[4] S. Vazquez-Rodriguez, M.J. Matos, F. Borges, E. Uriarte, L. Santana, Curr. Top. Med. Chem. 15 (2015) 1755–1766.
[5] S. Rahimi, S. Khoee, M. Ghandi, Carbohydr. Polym. 201 (2018) 236–245.
[6] A.A. Esenpınar, A.R. Özkaya, M. Bulut, J. Organomet. Chem. 696 (2011) 3873–3881.
[7] B.Z. Kurt, N.O. Kandas, A. Dag, F. Sonmez, M. Kucukislamoglu, Arab. J. Chem. (2017). https://doi.org/10.1016/j.arabjc.2017.10.001.
[8] D.M. Tian, F.F. Wang, M.L. Duan, L.Y. Cao, Y.W. Zhang, X.S. Yao, J.S. Tang, J. Agric. Food Chem. 67 (2019) 1937–1947.
[9] R. Teimuri-Mofrad, S. Esmati, S. Tahmasebi, M. Gholamhosseini-Nazari, J. Organomet. Chem. 870 (2018) 38–50.
[10] P. Thasnim, D. Bahulayan, New J. Chem. 41 (2017) 13483–13489.
[11] Y. Sert, M. Gümüş, H. G€okce, I. Kani, I. Koca, J. Mol. Struct. 1171 (2018) 850–866.
[12] A. Ibrar, S. Zaib, I. Khan, Z. Shafique, A. Saeed, J. Iqbal, J. Taiwan. Inst. Chem. Eng.. 81 (2017) 119–133.
[13] M.A. Köksoy, B. Köksoy, M. Durmuş, M. Bulut, J. Organomet. Chem. 822 (2016) 125–134.
[14] O.J. Jesumoroti, Faridoon, D. Mnkandhla, M. Isaacs, H.C. Hoppe, R. Klein, Med. Chem. Commun. 10 (2019) 80–88.
[15] L. Chen, L.L. Wu, W.J. Duan, T. Wang, L.T. Li, K.K. Zhang, J.M. Zhu, Z. Peng, F. Xiong, J. Org. Chem. 83 (2018) 8607–8614.
[16] L.H. Li, L. Chen, Y.F. Xia, J. China Pharm. Univ. 44 (2013) 374–379.
[17] S.P. Yang, L.J. Han, Y. Pan, D.Q. Wang, Y.N. Zhou, F. Zhang, Sci. China, Ser. B 43 (2013) 858–868.
[18] J.J. Zhu, J.G. Jiang, Mol. Nutr. Food Res. 62 (2018) 1701073.
[19] P. López-Rojas, M. Janeczko, K. Kubiński, Á. Amesty, M. Masłyk, A. Estévez-Braun, Molecules 23 (2018) 199.
[20] H.A. El-Sherief, G.E.-D.A. Abuo-Rahma, M.E. Shoman, E.A. Beshr, R.M. Abdel-baky, Med. Chem. Res. 26 (2017) 3077–3090.
[21] A. Bisi, C. Cappadone, A. Rampa, G. Farruggia, A. Sargenti, F. Belluti, R.M.C. Di Martino, E. Malucelli, A. Meluzzi, S. Iotti, S. Gobbi, Eur. J. Med. Chem. 127 (2017) 577–585.
[22] Y. Wang, P. Pigeon, S. Top, J.S. García, C. Troufflard, I. Ciofini, M.J. McGlinchey, G. Jaouen, Angew. Chem. Int. Ed. 58 (2019) 8421–8425.
[23] M. Beaupérin, D. Polat, F. Roudesly, S. Top, A. Vessières, J. Oble, G. Jaouen, G. Poli, J. Organomet. Chem. 839 (2017) 83–90.
[24] J.A. Carmona-Negrón, A. Santana, A.L. Rheingold, E. Meléndez, Dalton Trans. 48 (2019) 5952–5964.
[25] C.H. Mu, K.E. Prosser, S. Harrypersad, G.A. MacNeil, R. Panchmatia, J.R. Thompson, S. Sinha, J.J. Warren, C.J. Walsby, Inorg. Chem. 57 (2018) 15247–15261.
[26] B. Deka, A. Bhattacharyya, S. Mukherjee, T. Sarkar, K. Soni, S. Banerjee, K.K. Saikia, S. Deka, A. Hussain, Appl. Organomet. Chem. 32 (2018) 4287.
[27] T. Stringer, R. Seldon, N. Liu, D.F. Warner, C. Tam, L.W. Cheng, K.M. Land, P.J. Smith, K. Chibale, G.S. Smith, Dalton Trans. 46 (2017) 9875–9885.
[28] F. Fus, Y. Yang, H.Z.S. Lee, S. Top, M. Carriere, A. Bouron, A. Pacureanu, J.C. da Silva, M. Salmain, A. Vessières, P. Cloetens, G. Jaouen, S. Bohic, Angew. Chem. Int. Ed. 58 (2019) 3461–3465.
[29] E. Ketata, A. Neifar, W. Mihoubi, P. Pigeon, H. Gouzi, J.M. Mallet, S. Top, G.K. Gupta, G. Jaouen, A. Gargouri, M.E. Arbi, J. Organomet. Chem. 848 (2017) 133–141.
[30] X. Narváez-Pita, A.L. Rheingold, E. Meléndez, J. Organomet. Chem. 846 (2017) 113–120.
[31] B. Li, Q.X. Liu, Y.Q. Zhou, Z.D. Jia, M.Y. Zhu, Y. Xu, M.P. Song, Chin. J. Org. Chem. 37 (2017) 2008–2014.
[32] C. Wang, R.S. Jang, F. Feng, G.L. Fu, Chem. Reag. 30 (2008) 935–936.
[33] M.H. Li, J. Wang, S.D. Fang, Z.L. He, Chin. J. Spectrosc. Lab. 18 (2001) 796–798.
[34] D.T. Wang, Y.P. Wang, Mater. Sci. Technol. 13 (2005) 662–664.
[35] R.L. Sun, L. Wang, H.J. Yu, A. Zain ul, Y.S. Chen, H. Khalid, N. Abbasi, M. Akram, J. Inorg. Organomet. Polym. 24 (2014) 1063–1069.
[36] P.P. Xu, X.N. Liu, X. Zhao, W.J. Zhu, M. Fang, Z.Y. Wu, L.C. Du, C. Li, J. Chin. Chem. Soc. (2019) 1–8.
[37] X.M. Peng, K.V. Kumar, G.L.V. Damu, C.H. Zhou, Sci. China Chem. 59 (2016) 878–894.
[38] E.H. Avdovića, D.L. Stojkovića, V.V. Jevtića, D. Milenkovićb, Z.S. Markovićb, N. Vukovića, I. Potočňákd, I.D. Radojeviće, L.R. Čomiće, S.R. Trifunovića, Inorg. Chim. Acta 484 (2019) 52–59.
[39] W.D. Zhou, L. Wang, H.J. Yu, X. Xia, Appl. Organomet. Chem. 32 (2018) 3932.
[40] F. Asghar, S. Fatima, S. Rana, A. Badshah, I.S. Butlerc, M.N. Tahird, Dalton Trans. 47 (2018) 1868–1878.
[41] K.N. Chethan Prathap, N.K. Lokanath, J. Mol. Struct. 1171 (2018) 564–577.
[42] A. Satheshkumar, R. Manivannan, K.P. Elango, J. Organomet. Chem. 750 (2014) 98–106.
[43] J. Zheng, K.L. Wu, T.H. Shi, Y. Xu, Appl. Organomet. Chem. 27 (2013) 698–703.
[44] B.B. Zhou, J. Li, B.J. Feng, Y. Ouyang, Y.N. Liu, F.M. Zhou, J. Inorg. Biochem. 116 (2012) 19–25.